

# INVESTIGATING THE INFLUENCE OF URBAN GREEN SPACES ON URBAN HEAT ISLAND MITIGATION – TAKING FOUR DISTRICTS IN SHIJIAZHUANG AS AN EXAMPLE

Nan ZHANG<sup>1</sup>, Qiuning DING<sup>1</sup>, Haitao WANG<sup>1, 2</sup>✉

<sup>1</sup>*School of Architecture, Department of Architecture, Tianjin Chengjian University, No. 8, Health Road, 300384 Tianjin, China*

<sup>2</sup>*Tianjin Chengjian University, No. 8, Health Road, 300384 Tianjin, China*

## Highlights:

- the data are relatively new, using the latest remote sensing satellite imagery to study daily ambient temperatures rather than previous seasonal month comparisons;
- there are few literatures on Shijiazhuang, which can supplement the vacancy in this field;
- studying the impact of urban parks on cooling is more feasible for urban policy designers;
- when studying the impact of cooling, factors such as the density of surrounding buildings are taken into account, which will not be too limited;
- finally, the optimal cooling range is calculated, and the specific figures can be a favorable reference.

## Article History:

- received 17 June 2024
- accepted 10 December 2024

**Abstract.** The primary objective of this scholarly investigation is to elucidate the intricate interplay between the urban heat island (UHI) effect and municipal green spaces. The geographical focus includes the four areas with the highest urbanization rate in Shijiazhuang, China. To conduct this survey, ECOSTRESS remote sensing imagery was acquired during distinct temporal intervals—morning, midday, and evening. The data were collected using the equal-scale city blocks performed by the OpenStreetMap urban network and ECOSTRESS remote sensing images at different times (morning, noon and evening). Surface temperature inversion of satellite images was performed using ArcGIS 10.7 software to obtain surface temperature. The overarching aim was to discern the nuanced impact of urban parks on the surface temperatures of their proximate environs during the summer season. The findings of this investigation revealed that, in order to effectively ameliorate the discernible heat island effect (SUH), rejuvenation initiatives ought to be directed toward sites maintaining a distance from green spaces within the range of 160 to 370 meters. Furthermore, augmentation of green space configurations is recommended in vicinities characterized by building densities falling within the range of 0.2 to 0.3. Notably, in locales marked by high building density, park layouts should adhere to a more regularized design during the renovation process. Additionally, it is advisable to ensure that the spatial separation between distinct urban parks exceeds 900 meters. These empirical insights are poised to enhance the comprehension of urban planners regarding the intricate dynamics through which urban parks exert influence on municipal surface temperatures. Furthermore, the discerned patterns furnish pragmatic guidance for mitigating the heat island effect, thereby offering invaluable recommendations for urban planning endeavors.

**Keywords:** urban parks, surface temperature, heat island effect, cooling distance.

✉Corresponding author. E-mail: [wht007@tcu.edu.cn](mailto:wht007@tcu.edu.cn)

## 1. Introduction

Urban Heat Islands (UHI) are urbanized areas with higher temperatures than rural areas. Changes in surface material due to vegetation suppression, albedo changes and soil sealing affect the local energy balance and promote the formation of UHI in warmer seasons, an effect that leads to thermal discomfort, higher energy consumption and increased pollution effect (Almeida et al., 2021). Consequently, urban temperatures register higher values due to these combined factors. Notably, the influence of urban heat dissipation (Founda, 2011) emerges as particularly significant. In response to the imperatives posed by cli-

mate change and the UHI effect, a strategic augmentation of urban green spaces (Spronken-Smith & Oke, 1999; Cao et al., 2010), including park gardens, street trees, and green roofs (Armson et al., 2012), represents a viable mitigative approach. Presently, research on the nexus between the UHI effect and urban green spaces predominantly centers on vegetation classification and data analysis, with comparatively fewer investigations addressing the impact of spatial distances surrounding urban green spaces on their cooling efficacy.

The study showed that non-urban areas with vegetation cover, such as LCZB or LCZF, had significantly lower SUHI effect values under the same conditions. The

existence of green belt reduces the cold island effect of SUHI effect on the surrounding urban space (Errea et al., 2023). Therefore, this study attempts to use remote sensing technology to quantitatively analyze the cooling benefits of urban green space at different distances during different periods of day and night. The ultimate goal is to procure data that maximally encapsulates the cooling island effect of green spaces, furnishing a foundational reference for urban green space planning.

Existing studies on the cooling impact of urban parks on their vicinities primarily emphasize the ecological attributes intrinsic to the parks themselves and the dimensional characteristics thereof. Research conducted by Yang et al. underscores the significance of elements such as water bodies and green spaces in influencing the cooling island effect of urban parks (Yang et al., 2016). A case study in Tokyo, Japan, involving the measurement of air temperature, relative humidity, wind patterns, leaf temperature, and various surface temperatures, revealed that the majority of parks could achieve reductions in air temperature of approximately 1.5 degrees Celsius and meet 15 percent of their cooling energy requirements around midday. This underscores the pivotal role played by urban parks, particularly those featuring enhanced water or green space components, in generating a substantial cooling island effect within areas characterized by high building density and dense population (Peng et al., 2020; Yang et al., 2022). Subsequent research by Wang Xinjun et al. further elucidated various green space indicators, affirming that the optimal cooling effect is realized when park areas fall within the range of 1.34 to 17 hectares. The study found that a lower central park temperature correlates with a more potent cooling effect on surrounding structures and thoroughfares. Moreover, circular park layouts with a smaller perimeter-to-area ratio are deemed ideal for achieving optimal cooling effects. The study also underscored the contributory roles of water area, impervious surface reduction, and specific vegetation indices, such as leaf area index and tree cover, in influencing the cooling effect of urban parks. Notably, tree height and diameter at breast height (DBH) exhibited negligible impacts on the cooling effect, while dense vegetation configurations conferred appreciable cooling effects (Wang et al., 2018).

The UHI phenomenon manifests as an augmented surface temperature within a city, attributed to distinctive urban patterns characterized by high density and diminished environmental quality within specific locales. This leads to a pronounced diminution in the level of environmental thermal comfort (Mihalakakou et al., 2002). The mitigative potential of low building density, particularly in the context of high-rise structures, is underscored, as it serves to diminish heat source generation and enhance ventilation. Additionally, the relationship between urban surface temperature and morphological factors varies seasonally, as evidenced by a study conducted in the high urban density area of Beijing's Fifth Ring Road. The research disclosed that heightened building density corresponds to elevated surface temperatures, whereas an increase in the floor area

ratio and green space ratio within urban neighborhoods correlates with a reduction in surface temperature (Gobakis et al., 2011).

Furthermore, the cold island effect within urban parks is intricately linked to the park landscape, surroundings, and local climate (Mihalakakou et al., 2004; Livada et al., 2002). In regions experiencing cold climates, winter snowfall alters the surface characteristics of urban parks, albeit those with partially altered surface characteristics continue to exert some cooling effect in the absence or scarcity of snow accumulation. In locales dominated by snow and ice cover, however, no discernible correlation exists between urban green spaces and the UHI effect (Hamada et al., 2013). In areas characterized by limited water resources, low annual rainfall, or arid climates, water-dominated parks may not be conducive to mitigating the UHI effect, considering the associated water consumption and economic costs. Additionally, small parks constituting 20% of green space or featuring restricted space for water bodies may exhibit negligible cooling effects (Ruiz et al., 2022). Climatically, the urban park cold island effect demonstrates heightened sensitivity to factors such as rainfall, temperature, and solar radiation, with a diminishing effect observed with increasing temperature and rainfall. Consequently, selecting data ranges devoid of summer rainfall and low cloud density is imperative to yield more pronounced correlation findings.

The spatial relationship between the cooling effect of urban parks and their distance has garnered considerable scholarly attention. For instance, Huang et al. (2018) delineated the minimum alteration in the maximum cooling degree as the spatial extent of the cooling effect and conducted an exhaustive investigation. Guo et al. (2021) mapped the contour of the cooling extent of urban parks to characterize the degree of cooling by calculating the slope of the surface temperature map. Furthermore, Toparlar et al. (2018) introduced four indicators—namely, maximum cooling distance, maximum cooling area, cooling efficiency, and local cold island intensity—to quantify the cooling effect of urban parks. Numerous studies posit that the cooling effect of blue-green landscapes exhibits spatial variation in a nonlinear relationship (Lin et al., 2015). In essence, the maximum cooling distance or area remains constant, while the cooling curves per degree Celsius change in distance exhibit variability (Cheng et al., 2015).

In summary, the research domain pertaining to the cooling impact of urban parks is expansive, continuously evolving with the burgeoning integration of remote sensing image technology. Particularly noteworthy is the heightened cooling effect of urban parks during the summer season, evidenced by an average cooling degree of 1.65 °C, an average maximum temperature change of 7.5 °C, and a predominant cooling range of approximately 120 meters. In contrast, the winter cooling effect of urban parks is relatively limited, with an average cooling degree of 0.48 °C, an average maximum temperature change of 4.25 °C, and a principal cooling range of around 90 meters in the absence or minimal presence of snow (Du

et al., 2016). Despite this, extant research lacks comprehensive insights into the daily fluctuations of the thermal environment within urban parks. Time trends of LST and temperature data (from weather stations) are very similar ( $\rho > 0.7$ ), with temperatures remaining stable in summer and increasing at night in winter. There was a strong correlation between biophysical indicators and summer LST at 11 a.m. and 1 p.m. Therefore, remote sensing data is effective in measuring temperature change over time and can be applied to urban thermal environment investigation (Almeida et al., 2023). Therefore, this study aims to use the most advanced ECOSTRESS remote sensing image technology to obtain daily variation data of land surface temperature to study the relationship between daily variation and distance of cooling effect of urban parks in summer, and to provide a comprehensive analysis of these time patterns. In contrast to previous research focusing on seasonal differences, we find that the diurnal intervals between cooling and distance are shorter, making it easier to reveal general correlations between cooling effects and distance.

## 2. Study area and data

### 2.1. Regional overview

Over the preceding three decades, substantial advancements have been witnessed in the urban landscapes of eastern China (Li et al., 2004). Noteworthy among these are the three principal urban agglomerations: the Beijing-Tianjin-Hebei region, the Yangtze River Delta, and the Pearl River Delta. These locales represent pivotal study areas characterized by a rapid and pronounced pace of urbanization within the region. The influence of eastern Chinese cities on surface temperature increase during 1971–2010 is very obvious. By comparing the time series of annual, monthly average, maximum and minimum surface temperature in urban and rural areas, it can be seen that the warming trend in urban areas is significantly stronger than that in rural areas, and UHI effect has intensified in recent years (Liao et al., 2017). The current global average temperature is about 1 °C higher than before the Industrial Revolution and is expected to reach or exceed 1.5 °C over the next two decades (Intergovernmental

Panel on Climate Change, 2022). In 2020, the average annual daytime surface urban heat island intensity of 366 cities in the world was 1.1 °C higher than that of atmospheric cities, and the average annual night surface urban heat island intensity was 0.3 °C higher than that of atmospheric cities. The average annual surface urban heat island intensity during daytime is 0.6 °C higher than that at night, while the average annual atmospheric urban heat island intensity during daytime is lower than that at night (Du et al., 2021). From 1996 to 2019, the expansion of built-up areas in Shijiazhuang city significantly affected the urban thermal effect, showing that the heat island effect increased in the expansion direction of the extended built-up areas (Qin et al., 2022).

Among them, as a provincial capital city in the Beijing-Tianjin-Hebei city cluster, Shijiazhuang has experienced a particularly obvious increase in the number of hot days in summer in recent years. In 2010, the number of hot days of 40 °C or above reached 4 days, and in 2023, it reached 7 days. In addition, the four districts in Shijiazhuang, as the four most populous districts in the city, have the smallest area, far higher population density than other districts, and the highest urbanization level (Data are from China Meteorological Data network – <https://data.cma.cn/>). Therefore, this region is chosen as the focus of this study. Located in the southern part of Hebei Province, Shijiazhuang (Figure 1) lies at the junction of the Taihang Mountains and the North China Plain, characterized by a temperate monsoon climate. As per data retrieved from the China Meteorological Network, July, the hottest month of the year, with an average temperature of 36 °C, and August, with a maximum precipitation of 164.4 mm, are both in summer. Conversely, winter experiences cold and arid conditions characterized by clear skies and diminished precipitation. Yang Peng et al.'s statistical examination of the UHI effect in Shijiazhuang reveals that recent urbanization processes and population growth exert a substantial influence on the UHI effect in the region. Despite the absence of a significant increase in the average annual temperature, the intensity of the UHI, particularly during nighttime, has witnessed a marked escalation since 1990. There is an obvious UHI effect in Shijiazhuang during the daytime in summer. Furthermore, a high correlation between air temperature and surface temperature is observed during

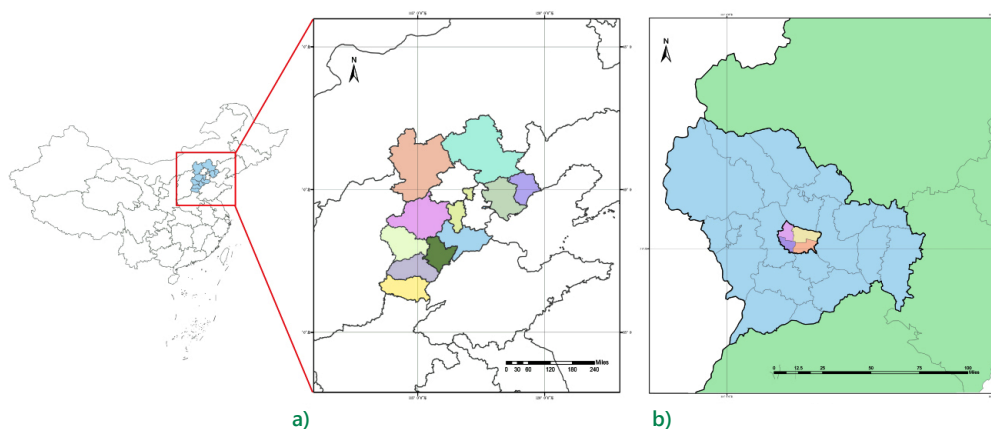


**Figure 1.** The location map of Shijiazhuang city is studied

nighttime, albeit to a lesser extent during daytime hours (Zhou et al., 2015).

In summation, the research findings underscore the close interrelation between the UHI effect and both surface and atmospheric temperatures. Additionally, the impact of winter snowfall on the urban subsurface is taken into consideration. The investigation primarily relies on remote sensing data during the months of July and August, selecting remote sensing images representative of key time periods throughout the day, namely 7 a.m., 12 noon to 2 p.m., 7 p.m., and 2 a.m., for the comprehensive analysis of the cooling dynamics within the buffer zone.

## 2.2. Data sources

The Ecosystems Onboard Thermal Radiometer Experiment (ECOSTRESS), deployed aboard the International Space Station in June 2018, represents an advanced satellite-based thermal imaging system. It possesses the capability to capture images of urban areas globally at various times throughout the day, approximately every 3–5 days, with a remarkable spatial resolution of 70×70 meters (Cai et al., 2017). This superior resolution, in contrast to traditional remote sensing platforms such as Landsat-8 (100×100 m spatial resolution) and MODIS (500×500 m spatial resolution), positions ECOSTRESS as a precise tool for monitoring the temporal evolution of the UHI effect, particularly in regions characterized by urban and non-urban interfaces (Shi et al., 2021). To mitigate interference from factors such as weather and soil moisture, ECOSTRESS remote sensing images were selected during periods with cloud cover below 5% around similar dates (July 15 to August 8), capturing morning, midday, and evening time points. This

selection enables a clearer and more comprehensive understanding of diurnal cooling trends in Shijiazhuang's parks. Figure 2 illustrates the ECOSTRESS images at different times during the summer in Shijiazhuang. In addition to ECOSTRESS data, this study leverages high-resolution images with a precision of 16×16 meters sourced from China's Gaofen-1 satellite. Furthermore, open-source data from Shijiazhuang city, obtained from OpenStreetMap (<https://www.openstreetmap.org>), has been utilized. The OpenStreetMap data facilitated the extraction of the city's road network and building contours, subsequently refined through ArcMap 10.7 to derive the distribution of city blocks. Manual acquisition of park vectors was also conducted to enhance the precision of the spatial data related to urban parks within the study area.

## 2.3. Selection of study parks

Urban parks are commonly recognized for their capacity to mitigate the UHI effect. In the pursuit of investigating the extent of cooling achieved by urban parks and discerning the correlation between their cooling efficacy and the surrounding urban morphology, this study focuses on ten selected parks in Shijiazhuang as the primary experimental subjects (Figure 3). In selecting parks, we aimed to avoid those influenced by factors such as nearby water bodies affecting cooling, extensive greenery within buffer zones, large shaded areas, and underlying surface materials. Therefore, parks meeting these criteria were preferably excluded from consideration:

1. A park with a large body of water around 300 meters (two blocks).

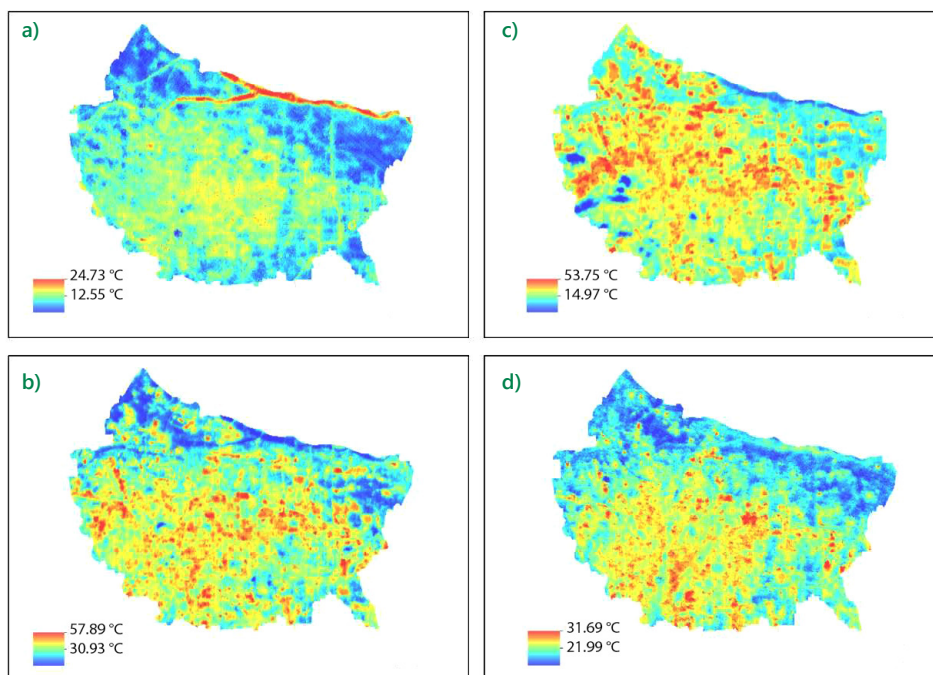


**Figure 2.** The spatial distribution feature map of land surface temperature in Shijiazhuang obtained from land surface temperature inversion calculation: a) at 22:23:04 on July 22, 2022 (clear sky); b) at 11:51:37 on August 8, 2022 (clear sky); c) at 14:14:37 on August 1, 2021 (clear sky); d) at 07:20:24 on July 15, 2020 (clear sky)

2. Avoidance of parks surrounded by substantial structures, such as viaducts, that may impart significant shading effects.
3. Elimination of parks featuring impervious non-green underlayment exceeding 50 percent of the total site area, encompassing materials such as hard paving.

By deliberately selecting parks with relatively straightforward environmental conditions based on these criteria, the research aims to enhance the precision of the investigation into the cooling impact of urban parks. This meticulous park selection process is designed to facilitate a more nuanced exploration of the intricate relationship between the cooling effects of urban parks and the prevailing characteristics of the surrounding urban landscape.

**Table 1.** City parks information sheet

Brochure	Park name	Perimeter (meters)	Area (square meters)
GS1	Dong Huan Park	1602.82	157241.38
GS2	Shi Ji Park	1590.15	160764.85
GS3	Menorah Park	1115.30	73289.33
GS4	Peace park	1821.67	182942.01
GS5	Tahrir Square	787.29	38177.44
GS6	Yu Xi Park	2198.88	278513.98
GS7	Water park	2832.22	331361.87
GS8	Xi Huan Park	1419.35	114865.75
GS9	Chang An Park	2372.49	289442.85
GS10	Railroad Culture Park	788.59	41995.06

### 3. Materials and methods

The predominant methodology in existing research examining the association between urban green spaces and LST relies on the grid method, wherein the study area is uniformly partitioned into spatial grids for analysis (Guo et al., 2019). However, such an approach, which categorizes urban space solely based on area size, lacks the requisite rigor and may overlook potential nuanced re-

lationships between surface temperature and the urban landscape. This globalized and undifferentiated research methodology may inadvertently neglect critical relationships, thereby hindering the effective implementation of research findings (Ke et al., 2021). In contrast, the city block, as the fundamental urban unit that materializes municipal plans and policies, emerges as a more nuanced and contextually relevant analytical unit (Montanges et al., 2015). Consequently, employing urban neighborhoods as the focal unit of investigation and discerning the diverse impacts of distinct spatial patterns on green spaces promise to deepen our comprehension of the role of green space in ameliorating the urban heat island effect (Tang et al., 2023). Therefore, this study will divide the study city Shijiazhuang into blocks and extract the influencing factors such as building density, floor area ratio and distance from green space of each unit. Subsequently, an analysis of the cooling effects on the adjacent parks and green spaces will be conducted to attain a more profound understanding of the intricate relationship between urban form and green space cooling.

To execute this, the city of Shijiazhuang will be systematically divided into neighborhoods by regularizing and refining the road network within the four districts of the city. Utilizing Geographic Information System (GIS), The city will be divided into plots and communities with nearly different shaped areas according to the road network. Concurrently, in tandem with the scrutiny of urban park characteristics, a selection of ten urban parks will serve as the focal points of research, as depicted in Figure 3 and Table 1. Employing ArcMap 10.7, the delineated vectors representing green spaces will be superimposed onto ECOSTRESS remote sensing images, facilitating the extraction of spatial distribution information pertaining to temperature both within and outside the bounds of the selected urban parks.

#### 3.1. Green space cooling study

To investigate the precise cooling range of urban parks, this study strategically establishes 34 buffer zones surrounding the selected urban parks at 30-meter intervals



**Figure 3.** a) shows the schematic of the selected park buffer; b) shows the study area; c) shows the distribution of the selected urban parks

based on the contours of the ten designated parks. The analysis aims to elucidate the temperature variation patterns within the vicinity of the urban parks, ranging from 0 to 990 meters, by examining the correlation between temperature and buffer distance. The methodology involves the superposition of layers to obtain the average surface temperature for each buffer zone (Figure 4). Subsequently, a statistical analysis is conducted, considering the distance from the park boundary and the average temperature as two variables for correlation analysis.

While many studies have traditionally employed Gaussian models for parametric analyses of cooling effects in parks, distance as features and the LST obtained from remote sensing images is processed by define surface inversion, these models assume that all observations within a specific category of these features adhere to a Gaussian distribution. Such studies often construct temperature-distance curves to identify common features of the cooling effect in parks (Anniballe et al., 2014). However, given the heightened spatial heterogeneity inherent in urban areas, the applicability of the average values derived from Gaussian models for estimating the cooling effect of parks may vary significantly.

Reduce the influence of temperature spatial continuity obtained from surface inversion, the analysis in this study concentrates on the average LST within both the parks and the buffer zones. The independent variable ' $r$ ' denotes the distance from the buffer zones to the park boundary, while the dependent variable ' $T$ ' represents the average LST of each buffer zone. The functional relationship of  $T$ - $r$  is then established through curve-fitting analysis, revealing that a cubic polynomial best characterizes this relationship (average  $R^2 = 0.937$ ). The cubic polynomial function  $T(r)$  is articulated as numerate the equations (Park et al., 2019):

$$T(r) = ar^3 + br^2 + cr + d.$$

In Figure 5, the fitted curve prominently illustrates the discernible relationship between the thermal environment of the parks and the respective distances. To quantitatively assess this relationship, we computed the disparity between the average surface temperature in varying buffer zones and the average temperature of the parks for comparative analysis, denoted as  $\Delta t$ . Table 2 delineates the diurnal variation of the maximum cooling amplitude



**Figure 4.** Schematic of the distribution of neighborhoods and their building density in the study area

observed across different parks. Notably, the maximum  $\Delta t$ , registering at 5.31 °C, is recorded at 14:14 in West Ring Park, while the minimum  $\Delta t$  of 0.01 °C is observed at 22:23 in Chang'an Park. The cumulative average  $\Delta t$  across all ten urban parks is calculated to be 1.37 °C.

This analysis provides a comprehensive overview of the daily temperature differentials within the buffer zones surrounding urban parks, highlighting variations in cooling amplitude at different times of the day across diverse park locations.

**Table 2.** Maximum diurnal variation in temperature drop (in °) from 0 to 990 m in selected urban parks

Brochure	Park name	07:20 (°C)	22:23 (°C)	14:14 (°C)	11:51 (°C)
GS1	Dong Huan Park	0.35	0.14	0.10	2.64
GS2	Shi Ji Park	0.33	0.58	2.52	3.47
GS3	Menorah Park	0.36	0.70	0.54	1.15
GS4	Peace park	0.20	0.32	1.50	2.04
GS5	Tahrir Square	0.22	0.28	0.26	2.19
GS6	Yu Xi Park	1.38	4.58	1.19	3.13
GS7	Water park	0.38	0.51	1.05	1.78
GS8	Xi Huan Park	0.19	0.76	5.31	2.57
GS9	Chang An Park	0.19	0.01	2.20	0.34
GS10	Railroad Culture Park	1.41	1.27	2.36	4.13

## 4. Results and analysis

### 4.1. Comparison of green space cooling

In order to ensure the referability of the experimental data, for each of the ten selected urban parks, using Arcmap10.7 software, the average surface temperature of each ring buffer was calculated by superimposing maps after rasterizing data. Subsequently, a fitting procedure was implemented, utilizing the distance from the boundary of the green space as the independent variable and the average temperature as the dependent variable. This method enabled the delineation of the cooling range pattern of urban parks. Comparative analyses were conducted by contrasting fitting results for the same parks at different times and different parks at the same time.

A salient observation pertains to the diurnal variation in the SUHI effect, a phenomenon that exhibits distinct patterns throughout the daily cycle. The intensity of the SUHI effect is more pronounced during daylight hours when solar radiation is robust, leading to a more substantial temperature differential (Sun et al., 2020). This trend was consistently evident across all ten selected urban parks. For instance, at 7:20, the temperature range within the city parks was recorded at 25.45~27.95 °C; by 11:51, this range expanded to 42.42~50.12 °C; at 14:14, the temperature range within the city parks spanned from 31.99~49.24 °C; and by 22:23, the temperature range was 14.93~20.92 °C.

These observations underscore the dynamic nature of the SUHI effect, emphasizing its heightened intensity during daylight hours and diminished influence at night when solar intensity is attenuated.

#### 4.2. Greenfield cooling curve analysis

The inflection points of the fitted curves obtained from buffer zones of varying widths exhibit distinct distances, with a notable trend indicating that larger buffer widths result in a diminished statistical description of the relationship between the two variables. A study by Sun et al. employed buffer zones of 300 meters, analyzing the relationship between green space cooling and distance. The study utilized the integration of the LST-distance function to derive a cooling index, yielding function curves akin to exponential functions. Notably, when the buffer strip width was set to 300 meters, the cooling effect of the park significantly exceeded the mathematical changes observed with a buffer width of 900 meters (Sun et al., 2020). In our

study, the approximate block width of 30 meters in four districts of Shijiazhuang city was selected as the buffer distance. Compared with the above studies, the smaller range of this distance can provide more reference data for our research to build mathematical models. Based on the findings illustrated in Figure 5, we can clearly observe significant differences in cooling benefits among different green spaces. Initially, we conducted statistical analyses of cooling effects based on experimental results.

The red curve (Figure 5) illustrates a linear plot depicting the cooling effect of urban parks versus distance in the early morning of summer. Notably, GS1, GS3, GS4, GS7, GS9, and GS10 exhibit discernible decreasing curves, suggesting that in the early morning of summer, closer proximity to the urban park correlates with a less pronounced cooling effect, and in some instances, a warming trend is observed. The cooling effect reaches its zenith at a distance of approximately 780 meters, with a subsequent tendency for the cooling effect to plateau as the distance continues to increase.

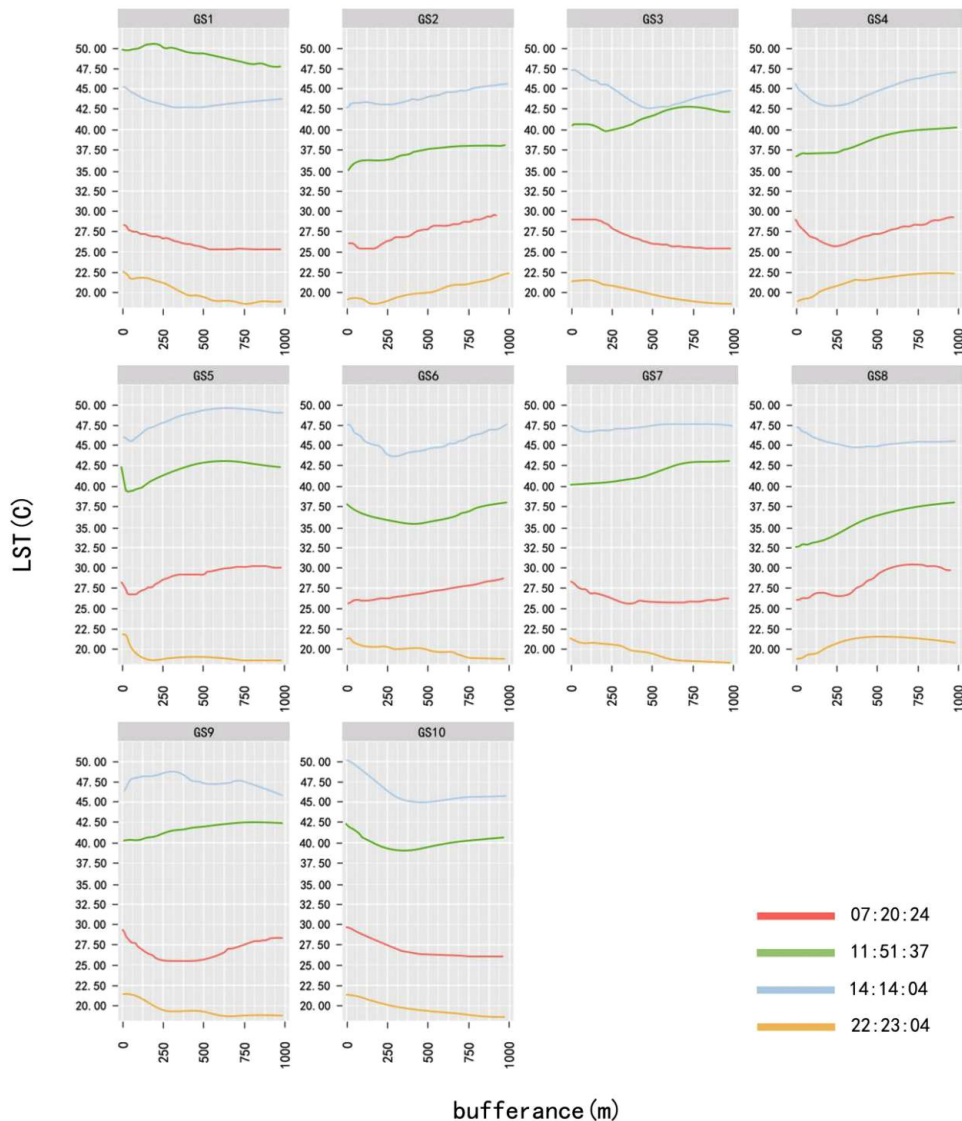


**Figure 5.** Line graph of daily changes in urban surface temperature around the ten selected urban parks, with the horizontal axis showing the distance of the buffer zone from the park (in m) and the vertical axis showing the surface temperature (in °C)

The green curve (Figure 5) portrays a linear plot of cooling versus distance for urban parks at midday in summer. GS2, GS3, GS4, GS5, GS7, GS8, and GS9 exhibit distinctive increasing curves, indicating that at midday in summer, the cooling effect diminishes as the distance from the city park increases, with the temperature effect leveling off around a distance of 800 meters.

The blue curve (Figure 5) illustrates a linear plot of urban park cooling versus distance in summer afternoons. GS1, GS2, GS4, GS6, GS8, and GS10 curves exhibit clear inflection points, transitioning from decreasing to increasing trends. This suggests that in summer afternoons, the distance effect on cooling in urban parks is most pronounced at 400–500 meters, with a subsequent warming phenomenon observed beyond 500 meters.

The yellow curve (Figure 5) presents a linear plot of cooling versus distance for urban parks in summer nights. GS1, GS3, GS7, and GS10 exhibit apparent decreasing curves, indicating that in summer nights, closer proximity to the city park correlates with a less pronounced cooling effect, and in certain instances, a warming trend is observed.

### 4.3. Maximum greenfield cooling

Finally a comparative study of the maximum cooling in city parks showed that the average park cooling  $\Delta t$  in Wrocław city ranged from 2.0 to 3.6 °C, from 0.7 to 2.2 °C in the 110 m range, and from 1.7 to 3.6 °C in the 1,000 m range, with a range of cooling from 110 m to 925 m (Zhang et al., 2022). The climate of Wrocław is Humid continental climates (Dfb). The green space in the center of Nanjing, which also has a temperate monsoon climate like Shijiazhuang, has a cooling range between 180 and 810 m, with an average of 540 m (Blachowski & Hajnyrch, 2021). The difference between the temperature of the buffer zone around the park and the average temperature of the park itself is denoted by  $\Delta t$ . At 7:20, it is in the range of 0.19~1.41 °C, which occurs at about 270 m distance from GS9 and 900 m distance from GS10, respectively; at 11:51,  $\Delta t$  is in the range of 0.34~4.13 °C, which occurs at about 300 m distance from GS9 and 450 m distance from GS10, respectively; and at 14:14,  $\Delta t$  is in the range of 0.11~5.31 °C, which occurs at about 960 m distance from GS1 at a distance of about 960 m and GS8 at a distance of about 990 m. At 22:23,  $\Delta t$  was in the range of 0.01~1.27 °C, occurring at GS9 at a distance of about 780 m and GS10 at a distance of about 990 m, respectively.

### 4.4. Building density and diurnal cooling around green spaces

It is not only the city's own green structure that affects LST and the temperature itself, but also the building indicators within city neighborhoods. Some scholars in Singapore have found that the intensity of urban heat emissions is highest when the land use types are commercial areas, high-density public housing areas and low-density resi-

dential areas (Quah & Roth, 2012). Considering from the point of view of park cooling, when the cold air cooling through the green space passes through the surrounding built-up area, both sides of the air will rapidly exchange heat, and a large temperature difference will form a large cooling range. When the BD (building density) around the green space exceeds a certain range, the circulation and diffusion of cold air will be blocked by the dense buildings, and this phenomenon leads to a reduction in the efficiency of the cooling effect of the green space (Zhang et al., 2022).

According to specify the parameters results of Arcmap10.7 on the building density of urban blocks, the BD of the built-up areas around the green areas is between 0 and 2, and the BD around Heping Park and Jiefang Square is the largest, 1.96. The BD of the plots about 600 meters away from the periphery of the parks is the smallest, 0. In order to preliminarily analyze the relationship between the BD and the cooling effect of the green areas, based on the value of the BD in the periphery of the built-up areas, all the periphery of the built-up areas are divided into 11 groups. Afterwards, the average cooling of the surrounding areas of these 11 groups of sample green spaces was counted, as shown in Table 3. Table 3 shows that there are 45 samples with BD in the range of 0.1~0.2, and the average temperature drop in the morning is 0.04 °C, which is the most obvious range interval for cooling, and there is 1 sample with BD in the range of 0.9~1.0, and the average temperature drop in the morning is -1.26 °C, which is the range interval with the worst cooling effect. We can preliminarily find that the cooling effect of the green space changes with the increase of BD in the surrounding area. In order to further analyze the cooling effect results during day and night, we analyzed the correlation between the surrounding BD of all green space samples and their cooling amplitude during day and night (Table 3).

**Table 3.** Grouping quantification of building density and diurnal cooling amplitude around green space

Building density (BD) (10,000 m <sup>2</sup> /ha)	Sample size	07:20 (°C)	22:23 (°C)	14:14 (°C)	11:51 (°C)
0~0.1	43	-0.05	0.28	0.99	1.32
0.1~0.2	45	0.04	0.14	0.72	0.54
0.2~0.3	90	-0.10	0.04	0.26	0.54
0.3~0.4	70	-0.17	0.22	-0.41	-0.23
0.4~0.5	45	-0.17	0.11	-0.59	0.46
0.5~0.6	26	-0.36	0.01	0.24	-0.04
0.6~0.7	17	-0.28	0.04	0.59	-0.35
0.7~0.8	8	0.01	0.36	-1.30	-0.27
0.8~0.9	3	-0.34	-0.11	-1.34	-1.67
0.9~1	1	-1.26	-0.41	-2.72	9.56
>1	8	-0.16	0.14	-0.49	-0.44

The comparative analysis conducted on the group disparities in the cooling amplitude of green spaces

concerning building density during both daytime and nighttime illuminates distinctive patterns. As observed in the preceding section, the cooling impact of green spaces is most pronounced during midday and afternoon, whereas mornings and evenings exhibit less conspicuous or, in certain instances, local warming phenomena. Figure 6 elucidates that within a building density (BD) range of 0~0.3, the cooling effect of green spaces is most conspicuous. As the BD surpasses 0.3, a discernible cooling effect is evident solely during the noon hours when solar radiation is at its zenith. When the BD exceeds 0.8, the cooling effect diminishes both during the day and night, with a notable fluctuation in the warming effect attributed to the limited sample size in this category. These findings provide valuable insights into the nuanced interplay between building density and the cooling dynamics of urban green spaces, emphasizing the temporal and spatial intricacies of this relationship.

## 5. Discussion

### 5.1. Cooling curves

In this study, the use of ECOSTRESS admin techniques facilitated the acquisition of daily cycle data on summer surface temperatures in urban parks and their adjacent buffer zones. In order to get the best cooling distance, we try to simulate the linear relationship between distance and cooling to get the inflection point between them. Consequently, preliminary findings indicate a discernible linear association between distance and cooling in the buffer zone surrounding city parks during the summer daily cycle. Specifically, during midday and afternoon periods in summer, proximity to the city park correlates with greater cooling effects, while during the early morning and nighttime intervals, closer proximity to the city park does not

manifest a significant cooling phenomenon, but rather exhibits a warming trend.

The study speculates that this phenomenon may be due to the fact that during the day, when there is plenty of sunlight, the plant's photosynthesis absorbs energy and releases water vapor, which causes the surrounding temperature to drop. However, stomatal conductance, often triggered by light, results in stomatal closure during nighttime hours, leading to reduced transpiration and increased net CO<sub>2</sub> emissions. Additionally, during the night, vegetation fails to provide shading, potentially contributing to the warming effect. These preliminary insights shed light on the intricate interplay between vegetation dynamics, ambient temperature, and the temporal aspects of the urban heat island phenomenon. Further research is warranted to delve into the underlying mechanisms and refine the understanding of these complex interactions.

### 5.2. Cooling trend fitting analysis

To validate the preceding analytical outcomes, we conducted an additional investigation into the functional relationship between the cooling amplitude of all green space samples and their respective distances. Subsequently, we attempted to apply the findings from existing studies to conduct curve fitting analysis. Figure 7 illustrates the fitting outcomes depicting the relationship between the distance surrounding green spaces and the cooling amplitude for the four distinct time periods throughout the entire day.

The curves derived from the fitting closely align with the trends identified in the earlier analysis. The fitting results reveal that both the diurnal and nocturnal variations in distance and green space perimeter temperature adhere to a cubic function. Specifically, as depicted in Figures 7a, 7b, and 7c, the temperature profile exhibits a decrease followed by an increase with distance during the daytime.

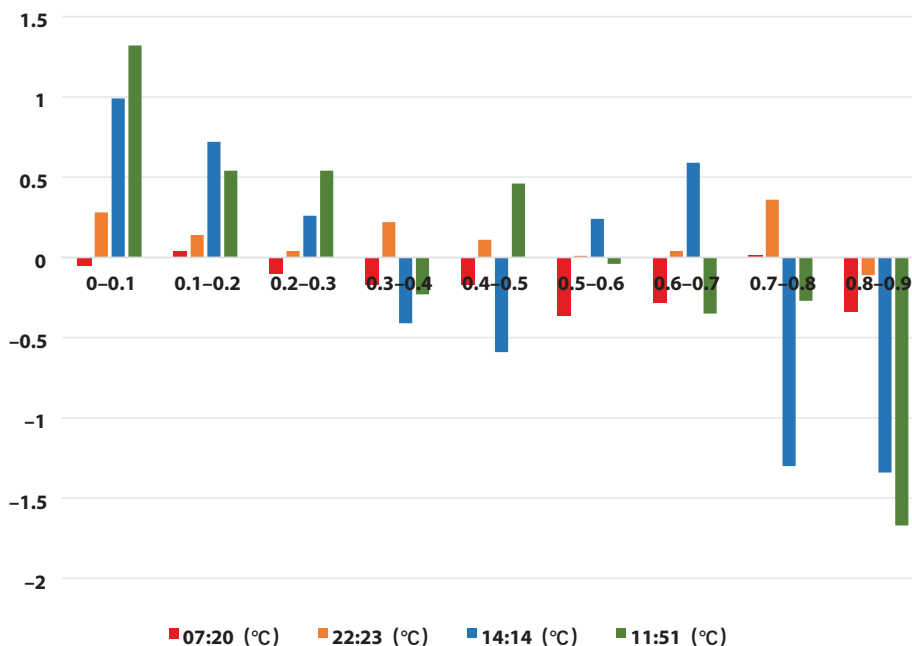


**Figure 6.** Quantitative comparison of building density and diurnal cooling magnitude grouped around green spaces

Conversely, Figure 7d indicates that during the nighttime, the temperature profile follows the opposite trend, increasing and then decreasing with distance. These findings provide further support for the proposed cubic function model, emphasizing the robustness and consistency of the observed patterns in the cooling effect of urban parks throughout the day and night.

Through the fitting of the three curves, a distinct inflection point in the temperature trend around the green space concerning distance becomes evident, and the directional shift around this inflection point is entirely opposite. This observation suggests that as the distance increases, the cooling effect of the green space diminishes. Simultaneously, the cooling effect of the green space is subject to various environmental factors in the surrounding area, including local climate conditions and built-up areas. In summary, the outcomes of this study reveal a degree of complexity and abruptness, emphasizing the multifaceted nature of the relationship between urban park cooling and its surrounding environment.

### 5.3. Maximum cooling distance

By fitting the inflection points present in the resulting three curves, we can find the maximum cooling distance. From Figure 7 shown in a, b, c and d we can get the maximum cooling distance for the four times of the day and night, the temperature is lowest in the morning at a distance of 365.67 m with 26.55 °C, in the middle of the day at a distance of 360.72 m with 45.36 °C, in the afternoon at a distance of 169.46 m with 38.95 °C, and in the evening at a distance of 811.62 m with 19.75 °C.

This means that the cooling effect of urban parks is more obvious in the distance from 160 meters to 370 meters. Compared with the cooling range of 110 to 925 meters in Wrocław (Blachowski & Hajnrych, 2021) and 180–810 meters in the central district of Nanjing (Quah & Roth, 2012), the cooling range of Shijiazhuang is even smaller. Therefore, in urban planning, it is necessary to reasonably arrange the distance between built-up areas and urban parks according to specific urban conditions, so as to alleviate the UHI effect.

In addition, by looking at the corresponding cooling amplitude of different urban parks, we found that the cooling effect of urban parks of the same size may differ in different urban morphologies. For example, GS9 is located in the city center, which is the area with the highest building density in the study area, and its cooling magnitude is low overall; while GS10 is located at the edge of the second ring road, with lower building density in the surrounding area, and its cooling magnitude is relatively high. This suggests that the cooling effect of urban parks does not only depend on their own area and perimeter, but the surrounding urban morphology also has some influence on them. These studies on cooling distance and building density can help us to plan and design urban parks more scientifically and determine the factors affecting the cooling effect of urban parks under different urban forms, so as to influence the planning of the distance between urban park layout and residential areas, and the formulation of design policies such as the selection of building design density around parks.

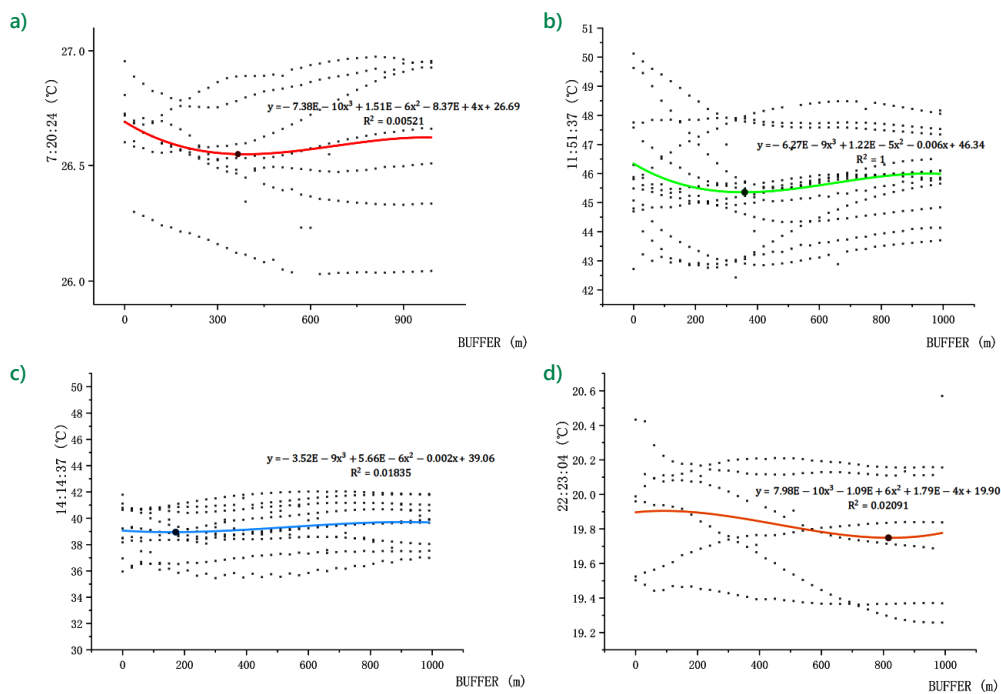


**Figure 7.** The fitting result between the surrounding distance of the green space and the cooling amplitude. The horizontal axis is the distance between the buffer zone and the park (unit: m), and the vertical axis is the surface temperature (unit: °C). The horizontal axis is the distance between the buffer zone and the park (unit: m), and the vertical axis is the surface temperature (unit: °C)

#### 5.4. Impact of built-up areas around green spaces

The built-up areas around green areas are mainly made of impervious concrete and asphalt surfaces such as residential areas, and the surfaces made of these materials often have higher heat capacity and lower reflectivity. Simultaneously, a higher concentration of buildings in the vicinity hinders air flow, diminishing the rate of heat exchange and consequently attenuating the cooling impact of the green space. Conversely, in locales featuring large and dense buildings, shadows cast tend to be more expansive, resulting in reduced ground radiation reception. Furthermore, areas characterized by less dense building arrangements, accompanied by strategically placed shading vegetation, can mitigate heat absorption. Therefore, a comprehensive assessment of the built-up area surrounding green spaces is imperative to comprehend the cooling effects during both daytime and nighttime. Additionally, careful consideration of the interplay between building structures and vegetation ratios within the built-up area is essential to optimize the cooling efficacy of the green space.

#### 6. Conclusions and recommendations

Based on the above study the following conclusions were obtained:

1. City parks in the daytime when the sunshine is sufficient for its surrounding environment can play a role in reducing the LST, alleviate the role of UHI effect, and with the increase in the distance of the effect is weakened; but in the early morning of the night in this type of no sunshine or insufficient sunshine, and there is no very obvious effect of temperature reduction.
2. The cooling amplitude of urban parks to the surrounding environment is the strongest in the afternoon, followed by the noon, and again in the

morning and the lowest at night, which corresponds to the day and night sunshine intensity.

3. Larger and regular shape of the city park cooling effect is more obvious, and the phenomenon embodied in the various parks on the different effects in the middle of the day is the most prominent.
4. There is a maximum cooling distance in urban parks. The maximum cooling distance in the morning is 365.67 meters; the maximum cooling distance at noon is 360.72 meters; the maximum cooling distance in the afternoon is 169.46 meters; and the maximum cooling distance at night is 811.62 meters (Figure 8).
5. The BD of the built-up area around the green space has an impact on the cooling effect of the surrounding green space, and its trend increases with the BD of the cooling effect is first enhanced and then reduced, and the cooling effect of the green space can be maximized in the range of 0.2~0.3.

By comparing Figure 3 and the current Google satellite map of Shijiazhuang City, it can be concluded that the large heat island effect is mainly concentrated in the second ring road of Shijiazhuang City, as well as in the southwest and northeast corners of the edge of Shijiazhuang City, and the land use of the key high-temperature areas is generally industrial in nature. Combined with the existing green space, it can be seen that there are fewer parks in the southwest and northeast corners of Shijiazhuang city, so it is recommended to increase the distribution of parks in this area to mitigate the heat island effect during planning. Planners can also rationalize park layout and residential design by the following design: It is recommended to plan urban built-up areas within 160–370 meters of the distance range where the heat island effect of urban parks is significant; In increasing the layout of the green space, choose the status quo for the temporary buildings or urban villages of low building density area for the nature of the land to change the density of the building to control the building to a maximum efficiency within the scope of

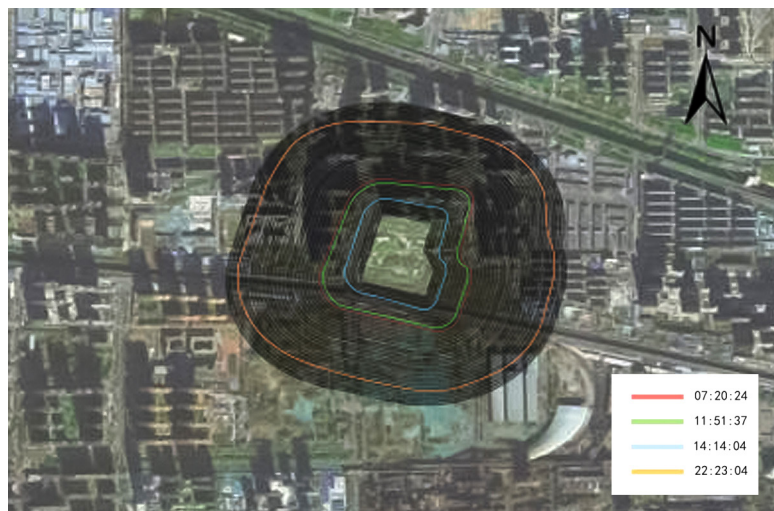


**Figure 8.** The diurnal variation of the optimal cooling range of the park taking Shi Ji Park as an example

the maximum. At the same time in the high building density area for transformation, should pay attention to the expansion of the park area and the shape of the regular. In this way, the urban heat island effect can be mitigated at the same time, so that the layout of the urban green space is more reasonable, and the benefits of planning and renovation can be maximized.

The results of this study can provide valuable reference for the urban development and ecological environment improvement of similar cities such as Shijiazhuang. However, the influence relationship between urban parks and surrounding built-up areas has not been further explored in the current research. In order to improve the research in this aspect in the future, the realization of urban site distribution planning may be combined with the research results. Finally, the thermal environment in urban areas can be effectively improved.

## Acknowledgements

The completion of this scientific study was made possible through the collaborative efforts and contributions of various individuals and organizations, for which we express our sincere gratitude.

We extend our appreciation to NASA for providing access to the Ecosystems Onboard Thermal Radiometer Experiment (ECOSTRESS) data, which served as a cornerstone in our research. The invaluable insights gained from these datasets significantly enriched our understanding of urban heat dynamics.

We would like to acknowledge the China Meteorological Network for furnishing essential climatic data that facilitated a comprehensive analysis of temperature trends in the study areas. Their commitment to data transparency and accessibility greatly contributed to the accuracy of our findings.

## Disclosure statement

The authors declare no conflicts of interest or financial disclosures that could potentially influence the objectivity or impartiality of this scientific study. This research was conducted with the primary aim of contributing to the academic and scientific community's understanding of urban heat island effects and the cooling dynamics of green spaces.

The study received no specific external funding, and the authors were not influenced or constrained by any external organizations in the design, implementation, or interpretation of the research findings. The scientific integrity of this study is maintained through adherence to rigorous research methodologies and ethical standards.

All data sources, including satellite imagery, climate data, and remote sensing information, were utilized in accordance with relevant licensing agreements, ethical guidelines, and legal regulations.

## References

- Almeida, C. R. d., Garcia, N., Campos, J. C., Alirio, J., Arenas-Castro, S., Gonçalves, A., Sillero, N., & Teodoro, A. C. (2023). Time-series analyses of land surface temperature changes with Google Earth Engine in a mountainous region. *Heliyon*, 9(8), Article e18846. <https://doi.org/10.1016/j.heliyon.2023.e18846>
- Almeida, C. R. d., Teodoro, A. C., & Gonçalves, A. (2021). Study of the Urban Heat Island (UHI) using remote sensing data/techniques: A systematic review. *Environments*, 8(10), Article 105. <https://doi.org/10.3390/environments8100105>
- Anniballe, R., Bonafoni, S., & Pichierri, M. (2014). Spatial and temporal trends of the surface and air heat island over Milan using MODIS data. *Remote Sensing of Environment*, 150, 163–171. <https://doi.org/10.1016/j.rse.2014.05.005>
- Armson, D., Stringer, P., & Ennos, A. R. (2012). The effect of tree shade and grass on surface and globe temperatures in an urban area. *Urban Forestry & Urban Greening*, 11(3), 245–255. <https://doi.org/10.1016/j.ufug.2012.05.002>
- Blachowski, J., & Hajnrych, M. (2021). Assessing the cooling effect of four urban parks of different sizes in a temperate continental climate zone: Wrocław (Poland). *Forests*, 12(8), Article 1136. <https://doi.org/10.3390/f12081136>
- Cai, G., Liu, Y., & Du, M. (2017). Impact of the 2008 Olympic Games on urban thermal environment in Beijing, China from satellite images. *Sustainable Cities and Society*, 32, 212–225. <https://doi.org/10.1016/j.scs.2017.03.020>
- Cao, X., Onishi, A., Chen, J., & Imura, H. (2010). Quantifying the cool island intensity of urban parks using ASTER and IKONOS data. *Landscape and Urban Planning*, 96(4), 224–231. <https://doi.org/10.1016/j.landurbplan.2010.03.008>
- Cheng, X., Wei, B., Chen, G., Li, J., & Song, C. (2015). Influence of park size and its surrounding urban landscape patterns on the park cooling effect. *Journal of Urban Planning and Development*, 141(3). [https://doi.org/10.1061/\(ASCE\)UP.1943-5444.0000256](https://doi.org/10.1061/(ASCE)UP.1943-5444.0000256)
- Du, H., Song, X., Jiang, H., Kan, Z., Wang, Z., & Cai, Y. (2016). Research on the cooling island effects of water body: A case study of Shanghai, China. *Ecological Indicators*, 67, 31–38. <https://doi.org/10.1016/j.ecolind.2016.02.040>
- Du, H., Zhan, W., Liu, Z., Li, J., Li, L., Lai, J., Miao, S., Huang, F., Wang, C., Wang, C., Fu, H., Jiang, L., Hong, F., & Jiang, S. (2021). Simultaneous investigation of surface and canopy urban heat islands over global cities. *ISPRS Journal of Photogrammetry and Remote Sensing*, 181, 67–83. <https://doi.org/10.1016/j.isprsjprs.2021.09.003>
- Errea, C. L., Almeida, C. R. d., Gonçalves, A., & Teodoro, A. C. (2023). Remote sensing analysis of the surface urban heat island effect in Vitoria-Gasteiz, 1985 to 2021. *Remote Sensing*, 15(12), Article 3110. <https://doi.org/10.3390/rs15123110>
- Founda, D. (2011). Evolution of the air temperature in Athens and evidence of climatic change: A review. *Advances in Building Energy Research*, 5(1), 7–41. <https://doi.org/10.1080/17512549.2011.582338>
- Gobakis, K., Kolokotsa, D., Synnefa, A., & Saliari, M. (2011). Development of a model for urban heat island prediction using neural network techniques. *Sustainable Cities and Society*, 1(2), 104–115. <https://doi.org/10.1016/j.scs.2011.05.001>
- Guo, G., Wu, Z., & Chen, Y. (2019). Complex mechanisms linking land surface temperature to greenspace spatial patterns: Evidence from four southeastern Chinese cities. *Science of the Total Environment*, 674, 77–87. <https://doi.org/10.1016/j.scitotenv.2019.03.402>

- Guo, J., Niu, H., Xiao, D., Sun, X., & Fan, L. (2021). Urban green-space water-consumption characteristics and its driving factors in China. *Ecological Indicators*, 130, Article 108076. <https://doi.org/10.1016/j.ecolind.2021.108076>
- Hamada, S., Tanaka, T., & Ohta, T. (2013). Impacts of land use and topography on the cooling effect of green areas on surrounding urban areas. *Urban Forestry & Urban Greening*, 12(4), 426–434. <https://doi.org/10.1016/j.ufug.2013.06.008>
- Huang, M., Cui, P., & He, X. (2018). Study of the cooling effects of urban green space in Harbin in terms of reducing the heat island effect. *Sustainability*, 10(4), Article 1101. <https://doi.org/10.3390/su10041101>
- Intergovernmental Panel on Climate Change. (2022). *Climate change 2022: Impacts, adaptation, and vulnerability. Contribution of working group II to the sixth assessment report of the intergovernmental panel on climate change*. Cambridge Press. <https://doi.org/10.1017/9781009325844>
- Ke, X., Men, H., Zhou, T., Li, Z., & Zhu, F. (2021). Complex mechanisms linking land surface temperature to greenspace spatial patterns: Evidence from four southeastern Chinese cities. *Urban Forestry & Urban Greening*, 62, Article 127159.
- Li, Q., Zhang, H., Liu, X., & Huang, J. (2004). Urban heat island effect on annual mean temperature during the last 50 years in China. *Theoretical and Applied Climatology*, 79, 165–174. <https://doi.org/10.1007/s00704-004-0065-4>
- Liao, W., Wang, D., Liu, X., Wang, G., & Zhang, J. (2017). Estimated influence of urbanization on surface warming in Eastern China using time-varying land use data. *International Journal of Climatology*, 37(7), 3197–3208. <https://doi.org/10.1002/joc.4908>
- Lin, W., Yu, T., Chang, X., Wu, W., & Zhang, Y. (2015). Calculating cooling extents of green parks using remote sensing: Method and test. *Landscape and Urban Planning*, 134, 66–75. <https://doi.org/10.1016/j.landurbplan.2014.10.012>
- Livada, I., Santamouris, M., Niachou, K., Papanikolaou, N., & Mihalakakou, G. (2002). Determination of places in the great Athens area where the heat island effect is observed. *Theoretical and Applied Climatology*, 71, 219–230. <https://doi.org/10.1007/s007040200006>
- Mihalakakou, G., Flocas, H. A., Santamouris, M., & Helmis, C. G. (2002). Application of neural networks to the simulation of the heat island over Athens, Greece, using synoptic types as a predictor. *Journal of Applied Meteorology*, 41(5), 519–527. [https://doi.org/10.1175/1520-0450\(2002\)041<0519:AONNTT>2.0.CO;2](https://doi.org/10.1175/1520-0450(2002)041<0519:AONNTT>2.0.CO;2)
- Mihalakakou, G., Santamouris, M., Papanikolaou, N., Cartalis, C., & Tsangrassoulis, A. (2004). Simulation of the urban heat island phenomenon in Mediterranean climates. *Pure and Applied Geophysics*, 161, 429–451. <https://doi.org/10.1007/s00024-003-2447-4>
- Montanges, A. P., Moser, G., Taubenböck, H., Wurm, M., & Tuia, D. (2015). Classification of urban structural types with multisource data and structured models. In *2015 Joint Urban Remote Sensing Event (JURSE)* (pp. 1–4), Lausanne, Switzerland. <https://doi.org/10.1109/JURSE.2015.7120489>
- Park, C. Y., Lee, D. K., Asawa, T., Murakami, A., Kim, H. G., Lee, M. K., & Lee, H. S. (2019). Influence of urban form on the cooling effect of a small urban river. *Landscape and Urban Planning*, 183, 26–35. <https://doi.org/10.1016/j.landurbplan.2018.10.022>
- Peng, J., Liu, Q., Xu, Z., Liu, D., Du, Y., & Qiao, R. (2020). How to effectively mitigate urban heat island effect? A perspective of waterbody patch size threshold. *Landscape and Urban Planning*, 202, Article 103873. <https://doi.org/10.1016/j.landurbplan.2020.103873>
- Qin, L., Liu, H., Shang, G., Yang, H., & Yan, H. (2022). Thermal environment effects of built-up land expansion in Shijiazhuang. *Land*, 11(7), Article 968. <https://doi.org/10.3390/land11070968>
- Quah, A. K. L., & Roth, M. (2012). Diurnal and weekly variation of anthropogenic heat emissions in a tropical city, Singapore. *Atmospheric Environment*, 46, 92–103. <https://doi.org/10.1016/j.atmosenv.2011.10.015>
- Ruiz, M. A., Colli, M. F., Martinez, C. F., & Correa-Cantaloube, E. N. (2022). Park cool island and built environment. A ten-year evaluation in Parque Central, Mendoza-Argentina. *Sustainable Cities and Society*, 79, Article 103681. <https://doi.org/10.1016/j.scs.2022.103681>
- Shi, H., Xian, G., Auch, R., Gallo, K., & Zhou, Q. (2021). Urban heat island and its regional impacts using remotely sensed thermal data—a review of recent developments and methodology. *Land*, 10(8), Article 867. <https://doi.org/10.3390/land10080867>
- Spronken-Smith, R. A., & Oke, T. R. (1999). Scale modelling of nocturnal cooling in urban parks. *Boundary-Layer Meteorology*, 93(2), 287–312. <https://doi.org/10.1023/A:1002001408973>
- Sun, X., Tan, X., Chen, K., Song, S., Zhu, X., & Hou, D. (2020). Quantifying landscape-metrics impacts on urban green-spaces and water-bodies cooling effect: The study of Nanjing, China. *Urban Forestry & Urban Greening*, 55, Article 126838. <https://doi.org/10.1016/j.ufug.2020.126838>
- Tang, L., Zhan, Q., Fan, Y., Liu, H., & Fan, Z. (2023). Exploring the impacts of greenspace spatial patterns on land surface temperature across different urban functional zones: A case study in Wuhan metropolitan area, China. *Ecological Indicators*, 146, Article 109787. <https://doi.org/10.1016/j.ecolind.2022.109787>
- Toparlak, Y., Blocken, B., Maiheu, B., & van Heijst, G. J. F. (2018). The effect of an urban park on the microclimate in its vicinity: A case study for Antwerp, Belgium. *International Journal of Climatology*, 38(S1), 303–322. <https://doi.org/10.1002/joc.5371>
- Wang, X., Cheng, H., Yang, J., Wang, X., & Zhao, Y. (2018). Relationship between park composition, vegetation characteristics and cool island effect. *Sustainability*, 10(3), Article 587. <https://doi.org/10.3390/su10030587>
- Yang, J., Guo, R., Li, D., Wang, X., & Li, F. (2022). Interval-thresholding effect of cooling and recreational services of urban parks in metropolises. *Sustainable Cities and Society*, 79, Article 103684. <https://doi.org/10.1016/j.scs.2022.103684>
- Yang, P., Xiao, Z.-N., & Ye, M.-S. (2016). Cooling effect of urban parks and their relationship with urban heat islands. *Atmospheric and Oceanic Science Letters*, 9(4), 298–305. <https://doi.org/10.1080/16742834.2016.1191316>
- Zhang, Q., Zhou, D., Xu, D., & Rogora, A. (2022). Correlation between cooling effect of green space and surrounding urban spatial form: Evidence from 36 urban green spaces. *Building and Environment*, 222, Article 109375. <https://doi.org/10.1016/j.buildenv.2022.109375>
- Zhou, D., Zhao, S., Zhang, L., Sun, G., & Liu, Y. (2015). The footprint of urban heat island effect in China. *Scientific Reports*, 5, Article 11160. <https://doi.org/10.1038/srep11160>